Informes de la Construcción
Vol. 73, 562, e398
abril-junio 2021
ISSN-L: 0020-0883
https://doi.org/10.3989/ic.79082

Building Reconstruction and Urban Analysis of Historic Centres with Airborne Photogrammetry

Reconstrucción de edificios y análisis urbanístico de centros históricos con fotogrametría aérea

Inmaculada Picon-Cabrera (*), Pablo Rodríguez-González (**), Isabella Toschi (***), Fabio Remondino (****), Diego González-Aguilera (*****)

ABSTRACT

Historical city centers are complex scenarios to be reconstructed in 3D. Advances in automated 3D reconstruction are useful to apply urban analysis that otherwise will require a lot of human effort. In this paper, urban parameters are automatically derived to quantify the urban analysis in historical city centers. Particularly, an aerial photogrammetric flight is used as input data to reconstruct 3D models of buildings with metric capabilities. The results reveal that geometric information of buildings (heights, areas and volumes) and urban density attributes (building coverage ratio and floor area ratio) plays an essential role in the design, planning and management of historical cities. The approach developed was validated in the historical city center of Trento (Italy) using cadastral data and a mobile mapping system (MMS) as ground-truth.

Keywords: Aerial photogrammetry, Building extraction, Complex geometries, Mobile Mapping System, Urban analysis.

RESUMEN

Los centros urbanos históricos son escenarios complejos para su reconstrucción tridimensional. Los avances en la reconstrucción automática son de gran utilidad para realizar análisis urbanísticos que de otra manera requerirían un elevado esfuerzo humano. En este artículo, se derivarán de forma automática parámetros urbanísticos para el análisis de los centros históricos. En particular, se utiliza un vuelo fotogramétrico como base para la obtención de modelos 3D de edificios con propiedades métricas. Los resultados revelan que la información geométrica de los edificios (alturas, áreas y volúmenes) y los atributos de densidad urbana (intensidad de ocupación del suelo en 2D y 3D) juegan un papel esencial en el diseño, planificación y gestión de los centros históricos. El enfoque propuesto fue validado en el centro histórico de la ciudad de Trento (Italia) utilizando datos catastrales y un sistema de cartografiado móvil como referencia geométrica.

Palabras clave: Fotogrametría aérea, extracción de edificios, geometrías complejas, sistemas de cartografiado móvil, análisis urbanístico.

(*) Bsc. Surveying. Associate professor. Higher Polytechnic School of Ávila – University of Salamanca, Ávila (Spain).
(**) PhD. Geodesy and Cartography. Assistant professor. University of León, Ponferrada (Spain).
(***) PhD in High Mechanics and Automotive Design & Technology. Researcher. 3DOM research unit – Bruno Kessler Foundation, Trento (Italy) and nFrames GmbH, Stuttgart (Germany).
(****) PhD in Photogrammetry. Full Professor. 3DOM research unit – Bruno Kessler Foundation, Trento (Italy).
(*****) PhD. Geodesy and Cartography. Full professor. Higher Polytechnic School of Ávila–University of Salamanca, Ávila (Spain).
Persona de contacto/*Corresponding author*: p.rodriguez@unileon.es (P. Rodríguez-González)
ORCID: http://orcid.org/0000-0002-7381-9346 (I. Picón-Cabrera); http://orcid.org/0000-0002-2657-813X (P. Rodríguez-González); http://orcid.org/0000-0002-6602-529X (I. Toschi); http://orcid.org/0000-0001-6097-5342 (F. Remondino); http://orcid.org/0000-0002-8949-4216 (D. González-Aguilera)

Cómo citar este artículo/*Citation:* Inmaculada Picon-Cabrera, Pablo Rodríguez-González, Isabella Toschi, Fabio Remondino, Diego González-Aguilera (2021). Building Reconstruction and Urban Analysis of Historic Centres with Airborne Photogrammetry. *Informes de la Construcción,* 73(562): e398. https://doi.org/10.3989/ic.79082

Recibido/*Received*: 11/04/2020
Aceptado/*Accepted*: 05/10/2020
Publicado on-line/*Published on-line*: 05/07/2021

1. INTRODUCTION

Historical urban centres constitute one of the most representative pieces in the landscape of our cities. Despite being a small part of the urban fabric, it constitutes a symbolic space that serves to identify, differentiate and give personality to cities (1). The city is in constant transformation, so the problem related to the conservation of the historical centres has to take into account that they act as regulators of their own transformations, both due to their own rigidity, and due to the social and morphological complexity that they accumulate (2). The experiences of conservation of historical centres are characterized, by the fact that the management and action models carried out lack of intervention criteria that incorporate the functional and territorial dimension, and in addition, these models are presented isolated from the city and the urban system of which they are part (3). By these reasons, the availability of detailed urban models of complex historical urban scenarios is of interest for urban managers and planners, which can provide more detailed analysis and urbanistic interventions (4).

The virtual urban modelling must face many challenges, not only the proper building modelling, but also the reconstruction of complex architectures and architectural heritage buildings, with their inherent difficulties (5). In fact, three-dimensional geographic information systems (GIS) in urban areas are increasingly becoming important in various applications, such as urban planning, urban policies and decision-making (6), as well as several transversal applications: environmental studies, simulation of pollution and noise, tourism, facility management, heritage conservation and management, damage assessment in emergencies (e.g. earthquakes, floods), telecommunications, or navigation systems in autonomous vehicles, among others.

Up to now, LiDAR has been the geomatic solution more common for building modelling and urban planning, due to the complexity associated to buildings, the presence of occlusions, shadows and non-visible areas (7). Several studies are focused on the use of LiDAR to derive 3D urban models, which are useful for urban planners to control the future directions of urban growth considering the availability of infrastructure (8-10)

The automatic reconstruction of urban 3D models has turned out to be one of the most growing sources of photogrammetric research in the last two decades. These automatisms or semi-automatisms seek to reduce costs in obtaining and processing data (11), offering a cost-effective means to obtain large-scale urban models. Additionally, recent developments of image-based methods encourage the use of image data (12). Photogrammetric based approaches are applied to different stages of urban modelling, as for instance the automatic building rooftop extraction for building reconstruction or solar energy supply (13); the generation of level of detail (LOD2) building models (12), the creation of digital city models based on aerial photogrammetry for the generation of 3D hydrodynamic models focused on flood simulations (14), or even, the estimation of building density using machine learning approaches over high-resolution remote sensing images (15). It is worth to highlight, the quickly growing sector of oblique airborne cameras (16, 17), with a potential for building façades reconstruction and accurate building footprint extraction (18, 19).

In this paper is presented an efficient and automatic workflow for the urban modelling of historical city centres using an airborne image system. The historical city of Trento (Italy) was taken as a case study.

1.1. Paper contributions

Given the abovementioned challenges and open issues, this article presents the following contributions:

- Novel approach for automated urban analysis.
- Procedure for the generation of 3D building models of historical urban centres.
- Challenging study case with narrow streets and complex historical buildings.
- Validation of the results against cadastral data and mapping mobile system measurements.

The paper is structured as follows: after this introduction, in Section 2 the geomatic sensors employed are detailed. In Section 3 the case study and data collection are described. In Section 4, the workflow developed is explained with special attention to building reconstruction. In Section 5 the experimental results of urban analysis (thematic urban maps, numerical urban coefficients and geometric data) are discussed. In Section 6, a comparison is established with a Mobile Mapping System (MMS) 3D point cloud in order to validate the results obtained. A last section is devoted to outline the main research contributions and to point out concluding remarks.

2. MATERIALS

Next the data sources employed in the study are presented. On one side, the aerial photogrammetric dataset and derived Digital Surface Model (DSM) that constitutes the input for the proposed building reconstruction process. On the other side, the MMS whose 3D model plays the role of ground truth to assess the quality of the building reconstruction.

2.1. Aerial photogrammetry

One of the main contributions of the following work is the use of a photogrammetric product to carry out the buildings' reconstruction, as well as the urban analysis derived, especially considering the complexity of historical centres.

The sensor employed is a Vexcel UltraCam Eagle digital camera, whose main technical specification are listed in Table 1.

Table 1. Main technical specification of the photogrammetric flight. Adapted from (20)

Parameter	Value
Image format	68.016 x 104.052 mm
Focal length	100.5 mm ± 0.002 mm
Pixel size	5.2 x 5.2 µm
Image size	13,080 x 20,010 px
Lens distortion	< 0.002 mm

2.2. Mobile mapping system

MMS systems offer a flexible solution in terms of accuracy, flexibility, point density and access to urban areas, bringing added value to record large and complex sites (21). A MMS

RIEGL (Table 2), that integrates two synchronously operated VQ-450 laser scanners, a portable control unit (VMX-450-CU) and IMU/GNSS navigation hardware, was used to document the main streets of the city centre of Trento. The system can measure up to 1.1 million points and 400 profiles per second, providing extremely dense and feature-rich data even at high driving speed. This MMS has been tested in a complex urban environment, bringing out its good metric potentialities (22).

Table 2. Technical specification of the RIEGL VMX-450. Adapted from (22)

Sensor	VQ-450
Measuring principle	Time of Flight
Laser wavelength	Near infrared
Laser measurement rate	300 – 1100 kHz
Maximum range	140 – 800 m
Minimum range	1.5 m
Accuracy	8 mm, 1σ
Precision	5 mm, 1σ
Sensor	IMU/GNSS
Absolute position	0.020 – 0.050 m
Roll and pitch	0.005 º
True heading	0.015 º
Sensor	VMX-450-CS6
Resolution	5 Mpx
Sensor size	2,452 x 2,056 px
Pixel size	3.45 µm
Nominal focal length	5 mm

3. CASE STUDY

3.1. Historical centre of Trento

The selected study site was the historical centre of Trento (Italy), located in the Italian Alps, with an approximate size of 3.5 km by 1.5 km. The city, with a population of about 117,000 inhabitants, lies on the banks of the river Adige, in the homonymous valley. It represents a complex urban scenario (Figure 1), encompassing historical building such as the Cathedral of San Vigilio in typical Romanesque style, the Medieval Palazzo Pretorio and some Renaissance buildings characterized by precious frescoed façades, without forget the typical narrow streets (average width of 3-4 m).

Figure 1. View of the study site. Source: (23)

3.2. Data collection

The dataset consisted of 397 images captured with the large-format nadir-looking digital camera UltraCamXp (Table 1). The image block was planned with a traditional 80/60 overlap (along/across track) and with an average ground sample distance (GSD) of 10 cm. The ground truth information for the aero-triangulation was based on 14 GPS-surveyed ground control points (GCPs) and 6 check points (CPs) acquired with a mean accuracy of 8 cm. Furthermore, the exterior imagery orientation parameters were available as GNSS-IMU observations.

The nadir imagery collected over Trento was processed using the traditional pipeline, consisting in aerial-triangulation (with self-calibration) followed by dense image matching and DSM generation (24). The output was a 2.5D point cloud resampled with a uniform spatial point distribution in the XY-plane. For more information related to the DSM computation please refer to (20).

The resulting DSM of the historical city centre of Trento was divided in six tiles (400 x 600 m) (Figure 2). The spatial resolution of the point cloud was of 0.1 m.

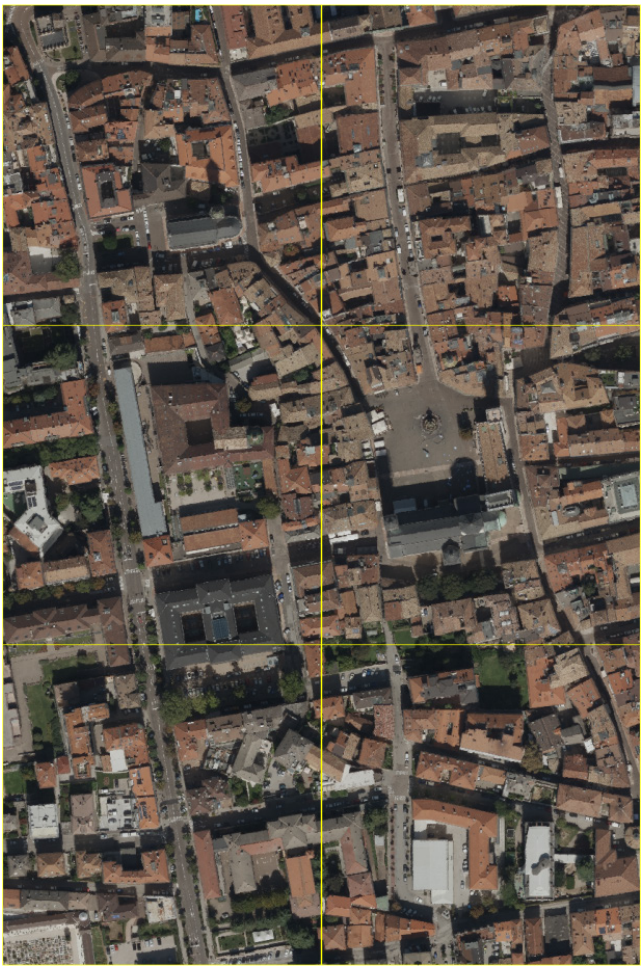

Figure 2. Aerial view of Trento including the six tiles analysed.

The number of tiles selected was limited to six, due to the computational cost of the proposed methodology. The processing was carried out in two different computers:

- Core I5 3570 3.4 GHz, 32 Gb of RAM, NVIDIA Quadro 4000: for all the filtering steps.
- Core I3 2100 3.1 GHz, 4 Gb of RAM: for Terrasolid execution due to license limitations.

The processing time was estimated around 3.5 – 4 hours per tile.

Regarding the MMS data collection, an area of about 700 m from west to east and of 500 m from north to south was covered in the city centre of Trento (Figure 3). The collected data was internally processed by RIEGL experts and finally delivered as point clouds (LAS file format) in WGS84 global coordinate system. The point clouds were characterized by a mean spatial resolution of 2-3 cm and were exported separately for each of the two mounted laser scanners.

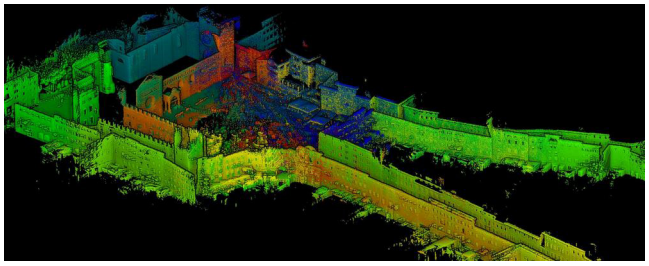

Figure 3. Detail of the 3D point cloud obtained with the MMS.

4. METHODOLOGY

Building extraction can be defined as the process to detect, structure, geometrically reconstruct and attribute building outlines and 3D models of buildings (25). Usually, software packages such as Terrasolid (26), requires a LiDAR point cloud in order to classify the point cloud into different classes (e.g. ground, building, vegetation, etc.) and then execute the building extraction. Since the input was a photogrammetric point cloud with a higher spatial resolution (2 pts/m²) than the LiDAR (100 pts/m²), it was necessary to filter the input point cloud in order to remove unnecessary information (e.g. façades, vegetation, cars, etc.) and classify them into two main classes: ground and building (i.e. roofs). To accomplish this, five pre-processing stages were applied, prior to the buildings' modelling (Figure 4).

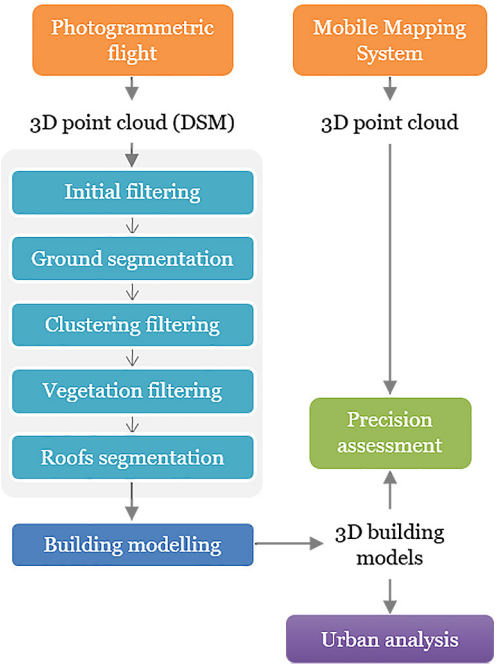

Figure 4. Workflow of the building reconstruction and urban analysis with airborne photogrammetry.

The summary of the software employed in the present methodology was:

- CloudCompare: visualization and data filtering.
- PCL/C++: data filtering and clustering.
- Matlab: data filtering.
- Microstation & Terrasolid: building modelling.

4.1. Filtering unnecessary information

The first stage (S1) removed those isolated points and the remaining façade points. The façade points were removed by a curvature analysis after a normal computation in CloudCompare (27), which is fully automatic. The isolated points were removed by a density filtering using a conservative threshold that could be defined accordingly to the spatial resolution (Figure 5).

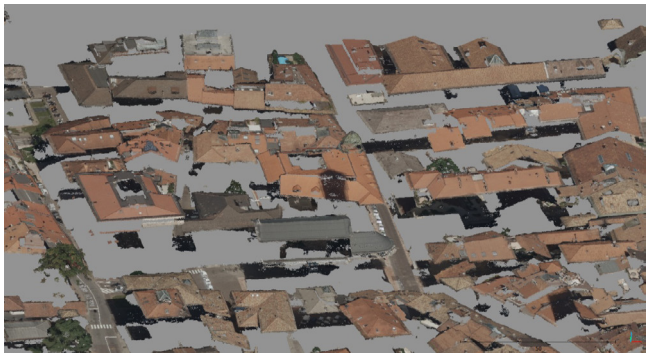

Figure 5. Filtering of unnecessary information (façades and isolated points).

4.2. Ground segmentation

The aim of the second stage (S2) was the ground classification. To do this, a progressive morphological filter segmentation (28) was applied by means of PCL library. It required four inputs:

- Maximum window size to be used in filtering ground returns.
- Slope value to be used in computing the height threshold.
- Initial height above the parameterized ground surface to be considered as a ground return.
- Maximum height above the parameterized ground surface to be considered as a ground return.

The parameters employed for the study case were:

- Maximum window size = 20 m
- Slope = 1
- Initial height = 0.5 m
- Maximum height = 3 m

As quality indicator, the 95.0 % of the points classified into the class "ground" belonged to the ground. The individual tile results are shown in the following table (Table 3). This evaluation was based on a visual inspection, since there was not a ground truth available.

Table 3. Assessment of "Ground" segmentation based on a visual inspection

Tile	Right	Wrong
6638_51040	96.8 %	3.2 %
6638_51038	94.7 %	5.3 %
6638_51036	96.5%	3.5 %
6640_51040	88.1 %	11.9 %
6640_51038	93.0 %	7.0 %
6640_51036	97.6 %	2.4 %

It should be remarked that in tile 6640_51040 the errors increased since these tiles correspond with narrow streets.

4.3. Clustering filtering

In this phase (S3), a clustering process was applied in the remaining points of the point cloud in order to remove those small point clusters, such as cars, vegetation, etc. (Figure 6). The clustering was carried out by the Euclidean Cluster Refinement (29) using PCL library. It required two inputs: the minimum number of points (which could be related to the spatial resolution) and the maximum distance to search the neighbour points (which is related to the spatial resolution and point cloud quality). In our case, a threshold of 2,000 points and maximum distance of 0.25 m were employed.

Figure 6. Point cloud after clustering filtering –S3. It should be remarked that still some roofs (corresponding to tents in terraces) and dense vegetation persist.

4.4. Vegetation filtering

By means of a Matlab (30) script the dense vegetation was removed (S4), especially the areas attached to the roofs (Figure 7). Since there was neither infrared information nor echoes for the vegetation classification common in LiDAR dataset, a combination of vegetation index and luminance was employed accordingly to an empirical threshold. This threshold was very sensible, since small fractions of roof points could be removed together with the vegetation.

Figure 7. Point cloud after vegetation filtering-S4. Big clusters of vegetation were removed as well as some minor roof points.

4.5. Roofs segmentation

Finally, a new clustering (S5) was applied to remove those small groups of vegetation that remain after stage S4. The filtering was the same of stage S3 (Euclidean Cluster Refinement). The remaining points were classified as "Building", assuming that all belong to roofs (Figure 8).

Figure 8. Final points of class "Building" after S5 filtering.

As a result of the 5-step filtering, the 96.7 % of the points were classified into the class 'building' belonged to roofs. Again, the assessment of roofs segmentation was based on visual inspection since a ground truth was not available. Results per tiles are outlined in Table 4:

Table 4. Assessment of "Roof" segmentation based on a visual inspection.

Tile	Right	Wrong
6638_51040	98.6 %	1.4 %
6638_51038	95.1 %	4.9 %
6638_51036	95.0%	5.0 %
6640_51040	99.2 %	0.8 %
6640_51038	97.1 %	2.9 %
6640_51036	93.6 %	6.4 %

4.6. Building modelling

Finally, both classes ('Ground' and 'Roofs') were introduced in Terrasolid (TerraScan and TerraModeler) (26) for the buildings model generation. The following parameters were setup:

- Maximum gap (3 m): Maximum distance between building parts belonging to the same model. If the distance is larger, separate building models are created.
- Merging tolerance (0.20 m): Additional tolerance for merging horizontal planes together.
- Minimum footprint (4 m²): Minimum size of a building footprint. This parameter is related with small roofs belonging to the same building.
- Maximum roof slope (75 deg): Maximum gradient of a roof plane.

In the following figure (Figure 9) is shown the final building modelling considering the parameters detailed above. Due to the hardware limitation, the six tiles were segmented into twelve city blocks.

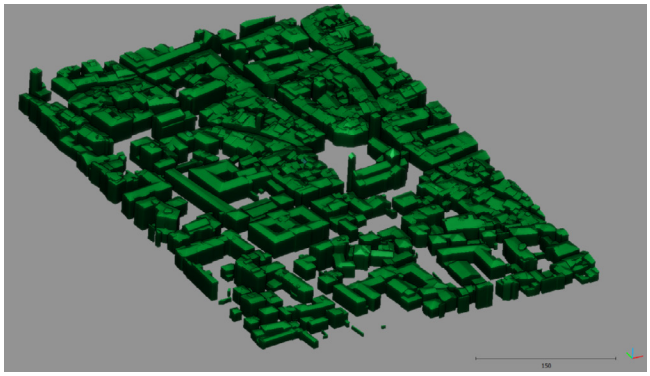

Figure 9. Perspective view of the buildings extracted for the modelling parameters.

As validation of the building modelling procedure and the error generated by the omission of eaves in the building footprint calculation, the total building area computed from our photogrammetric building modelling method was compared against the cadastral area of Trento (31) (Figure 10).

Figure 10. View of the selected cadastral elements for the building footprints computation.

Table 5. Comparison of average building footprint sizes obtained from cadastral data and from our photogrammetric-derived building models

Element	Total building area
Photogrammetric building modelling method	146,080.8 m²
Cadastre	135,524.5 m²
Discrepancy	+10,556.3 m²
Overall accuracy	92.2 %

The discrepancy between the cadastral and the photogrammetric-derived results is 7.8 %, in an area where the building area is 5,646.9 m2/ha (urban density). Please note that this discrepancy was caused by the omission of eaves together with the own error in building modelling.

5. URBAN ANALYSIS

Urban analysis plays an essential role in the design, planning and management of modern cities. To this end, an automated approach was developed to derive geometric urban information (heights, areas and volumes) and urban density attributes (building coverage ratio and floor area ratio) of buildings, land lots and urban units, using the photogrammetric-derived buildings models as input data.

Once the 3D modelling of buildings was performed, the following products are available:

- Digital Terrain Model-DTM (raster based on Ground segmentation-S2).
- Digital Surface Model-DSM (raster based on ground and roofs segmentation-S2+S5).
- Digital Building Model-DBM (vector based on 3D building modelling).

From that products and its combination, urban parameters can be extracted. In particular, the combination between raster DTM and vector DBM was required for obtaining correct building heights, since the façades provided by DBM use to penetrate under the terrain a minimum of 0.2 m. On the other hand, the DSM entailed volumetric problems, especially in buildings blocks, due to the triangulation between the roof

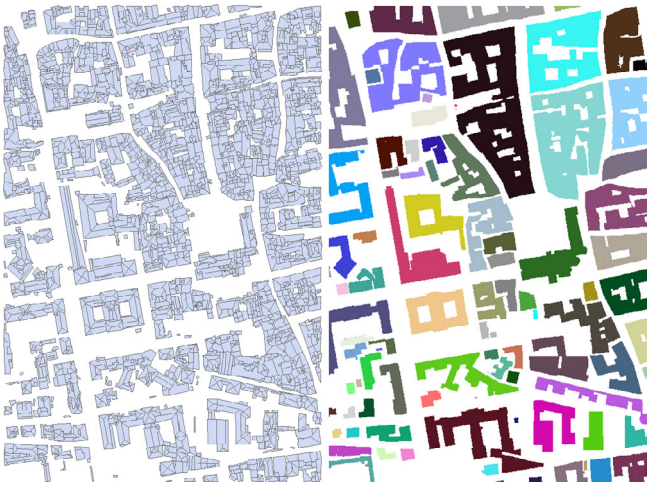

(a) (b)

Figure 11. (a) Vector building block layer with corrected. (b) Raster building block layer with corrected footprints.

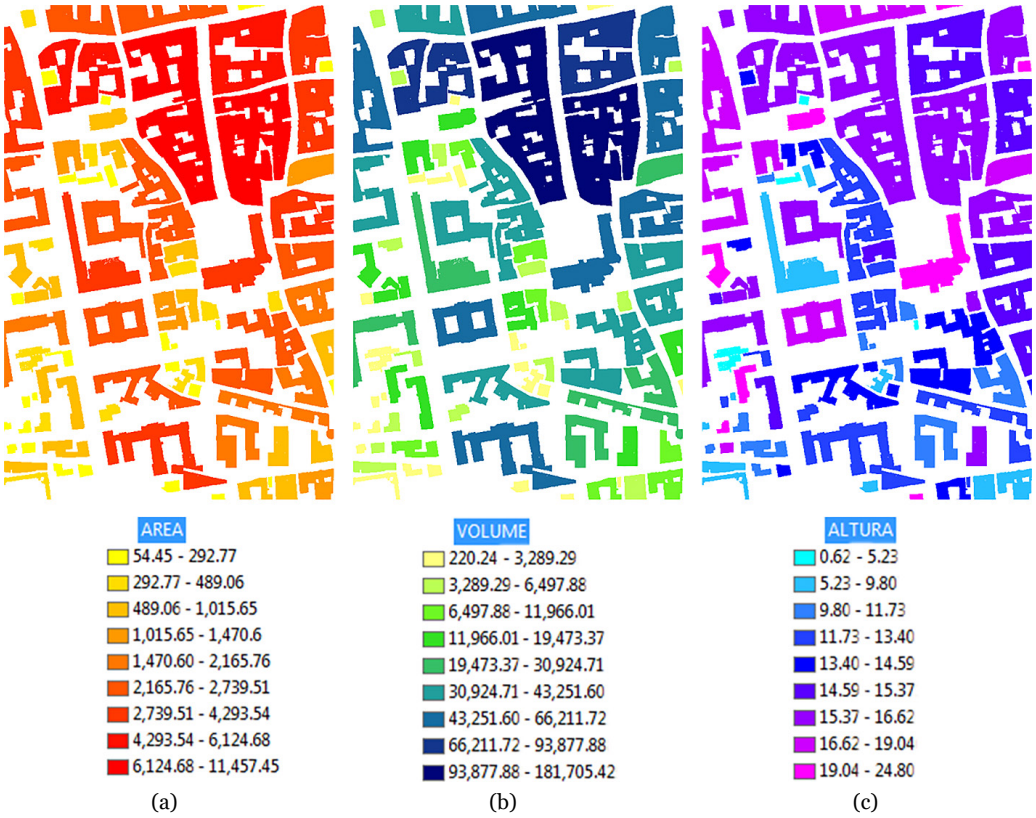

Figure 12. a) Area (m²) representation corresponding to building blocks; b) Volume (m³) representation corresponding to building blocks; c) Height (m) representation corresponding to buildings.

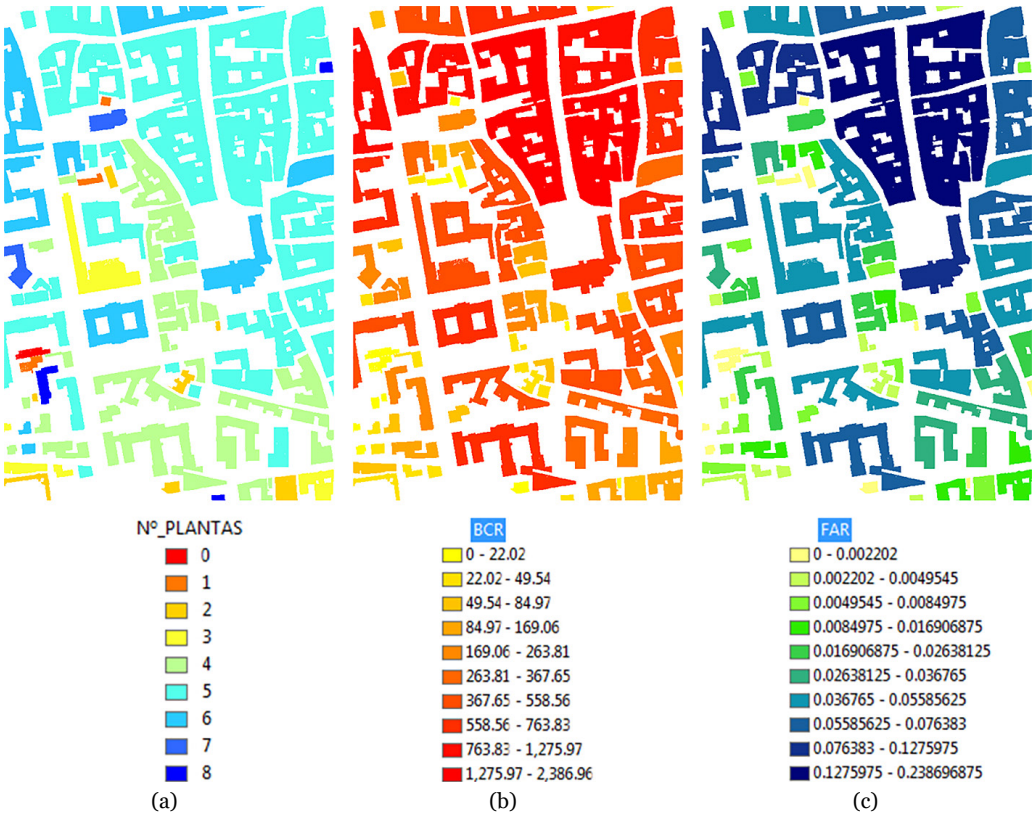

Figure 13. a) Number of floors per building block; b) Building density represented through the building coverage ratio-BCR parameter which outlines the number of square meters built per hectares or buildable area (m²/ ha); c) Suitability for building represented through the floor area ratio-FAR which outlines the surface occupation factor. This factor results from the ratio between the sum of the maximum built surfaces (including the number of floors) and the soil surface where the building is built.

and the ground. Therefore, the integration between DBM and DSM allowed us to correct this problem.

As a result of this combination (MDT-MDB; MDS-MDB), two layers which enclosed the correct heights (Figure 11) and footprints (Figure 11) for each building block were obtained.

Building density attributes can be expressed in 2D or 3D space through the Building Coverage Ratio (BCR) and Floor Area Ratio (FAR), respectively. The BCR measures the built meters in a hectare and is defined as the ratio of the building coverage area (i.e. the area of building footprint) to the size of land lot, as show equation [1]:

$$[1]\ BCR = \frac{\sum_{i=1}^{b} S_i}{S_L}$$

where ΣSi is the total building coverage area (in m²), and S_L is the area of land lot (in ha). Since the footprint represents the planimetric shape of a building, the BCR measures the building density in 2D space.

the FAR attribute is defined as the ratio of gross building floor area to the size of land lot, equation [2]):

$$[2]\ FAR = \frac{\sum_{i=1}^{b}\sum_{j=1}^{t} A_{i,j}}{S_L}$$

Based on these layers, geometric parameters (area, volume, height, etc.) and urban parameters (number of floors, floor area ratio-FAR and building coverage ratio-BCR) were automatically obtained corresponding to buildings blocks (Figure 12 and Figure 13).

This approach encloses a main problem since the geometric and urban parameters refer to building blocks. Trying to provide an urban analysis to individual buildings, the cadastral layer was used and crossed in order to solve this problem. As a result, the geometric and urban parameters could be assigned for each building (Figure 14).

Figure 14. Aerial view of Trento including the six tiles analysed.

In the following table (Table 6) is exemplified the geometric and urban parameters associated to each building of the historical centre of Trento (for space reasons not all the calculated values are listed).

Table 6. Geometric and urban parameters associated to each building.

Building ID	Volume (m³)	Area (m²)	Height (m)	Floors Nº	Built Surface (m²)	BCR	FAR
1	37122.4	2387.2	15.55	5	11935.8	497.3	0.0497
2	46805.2	2656.4	17.62	6	15938.6	664.1	0.0664
3	2785.3	138.7	20.08	6	832.1	34.7	0.0035
4	48753.7	3112.6	15.66	5	15562.8	648.5	0.0648
...	...	...	...	...	...	...	...
93	2666.7	109.2	24.43	8	873.4	36.4	0.0036

6. METHODOLOGY VALIDATION

For the methodology validation, eight building parts of the historical centre of Trento were selected. They corresponded to eaves clearly visible and identifiable, which were extracted from the DBM, the associated DTM and the MMS 3D point cloud. These areas were the following:

- Case 1: Building in the corner of streets Via delle Orfane and Via Roma.
- Case 2: Street Via Rodolfo Belenzani: Galleria Civica di Trento.
- Case 3: Building in the corner of streets Via Rodolfo Belenzani and Via Roma.
- Case 4: Building in the corner of Via dell Orfane and Piazza Diego Lainez. Eaves of the street (4P), and the ones oriented to the backyard (4S).
- Case 5: Building Torre della Tromba: superior battements (5S) and inferior eaves (5I).
- Case 6: Building in the corner of street Via Rodolfo Belenzani and Piazza Duomo.

The validation procedure was divided in two computations: (i) first, the height of the buildings was measured as a Z-axis increment. To this end, the building height was defined as the distance eave-ground; (ii) second, this distance was defined considering the possible height variations (i.e. ground slope).

In Table 7 is shown the spatial invariant, distance, among the eaves of selected buildings and the ground along the Z-axis for the DBM and the MMS point cloud. The values were computed using CloudCompare (27) and summarized on the basis of a Gaussian distribution (mean and standard deviation). The error is provided signed and percentual.

Table 7. Error assessment between DBM and MMS point cloud, by means of Z-axis discrepancy. Units: meters.

Case	MMS		DBM		Error	
	Mean	Std. dev.	Mean	Std. dev.		
1	16.44	± 0.04	16.07	± 0.15	-0.36	-2.2 %
2	15.13	± 0.05	14.89	± 0.03	-0.24	-1.6 %
3	15.83	± 0.08	15.46	± 0.24	-0.37	-2.3 %
4P	22.15	± 0.03	21.93	± 0.07	-0.23	-1.0 %
4S	22.29	± 0.05	22.20	± 0.11	-0.09	-0.4 %
5S	33.16	± 0.01	30.59	± 0.09	-2.57	-7.7 %
5I	32.03	± 0.03	30.85	± 0.09	-1.18	-3.7 %
6	17.05	± 0.06	16.67	± 0.07	-0.39	-2.3 %

In addition, the distance from the eaves to the ground along the ground's normal vector was also computed to consider the ground changes (Table 8).

Table 8. Error assessment between DBM and MMS point cloud according to the ground normal vector. Units: meters.

Case	MMS		DBM		Error	
	Mean	Std. dev.	Mean	Std. dev.		
1	16.45	± 0.05	16.10	± 0.17	-0.35	-2.12%
2	15.16	± 0.04	14.96	± 0.05	-0.20	-1.31%
3	15.85	± 0.09	15.51	± 0.22	-0.34	-2.13%
4P	22.17	± 0.04	21.96	± 0.04	-0.21	-0.97%
4S	22.25	± 0.02	22.23	± 0.07	-0.02	-0.11%
5S	33.15	± 0.03	30.66	± 0.12	-2.48	-7.49%
5I	32.03	± 0.04	30.91	± 0.11	-1.12	-3.49%
6	17.11	± 0.09	16.72	± 0.09	-0.39	-2.27%

For the assessment shown in Table 8, it was necessary to fit a plane to the nearest sidewalk of the building. Therefore, and due to the MMS acquisition error and constructive variations of the sidewalk, an additional error source was generated. The standard deviation of the plane fitting for all the study cases ranged between ±0.6 cm to ±2.8 cm, being the mean value ±1.3 cm. This amount is lower than the standard deviation of the distance eaves-ground, thus it is not considered as a significant error source that affect the abovementioned results.

Only the tower of case 5 (Torre della Tromba) shows a significant error of approximately 2.5 m and 1.1 m. These errors are caused due to the complexity of historical urban centres where the roofs of the buildings are unconventional.

Excluding this case, the mean discrepancy between the building height obtained by the proposed approached and the ground truth is around -0.3 m or a percentual error of -1.6 %. Considering that the 3D model provided by the aerial photogrammetry has a Z-axis RMSE of ±9 cm (20), and that the MMS precision is lower than ±1 cm (22), the error obtained is statistically significant and caused by the urban modelling approach. The percentual error is consistent with other building reconstruction studies, such as (7) where a relative error between 3.8 % and 6.9 % was obtained from LiDAR data.

It is worth to notice that the negative bias prevalent in the cases analysed could be related with the different point of view of data acquisition. Although the eaves of the buildings were selected to have the maximum visibility for aerial photogrammetry and MMS, the thickness of the eaves have undoubtedly influenced the comparison.

7. CONCLUDING REMARKS

3D building models offer an excellent dataset for automatized urban density analyses. In this paper, a novel approach, which makes use of 3D buildings models, provides an automated urban analysis of historical urban centres. This approach involves the use of aerial photogrammetric data to derive quantitative and qualitative urban parameters (the geometry and attributes of buildings), which are then analysed and validated against the ground-truth obtained from cadastral data and mapping mobile system measurements. Facing the 3D modelling of buildings in complex historical environments is a great challenge, especially if we seek to achieve automation and quality in the results. Various scripts were programmed in PCL and Matlab along with the use of commercial software to achieve the displayed results.

Many stakeholders of urban planning are unaware of the new possibilities open by modern photogrammetry and computer vision. In the case study tested we have demonstrated that geometric, volumetric and density attributes of buildings can be automatically derived from photogrammetric data. Specifically, the BCR estimator indicates the planimetric and horizontal density of buildings, while the FAR estimator indicates the 3D density of buildings. The following aspects of the approach developed and applied to the historical city of Trento can be highlighted:

- the possibility to automate urban analysis, which can facilitate regular, periodic performance of urban monitoring tasks.
- the accuracy and reliability of the information obtained, considering the validation carried out with cadastral and MMS data.
- the ability to access to inaccessible areas, especially those corresponding to narrow streets.

Despite the aforementioned improvements for urban management, the present approach shows limitations in areas of narrower or much denser streets, which can reduce the completeness of the final model due to the occlusions. To cope with severe occlusions in urban environments, the use of oblique photogrammetry should be combined with that of portable terrestrial mobile mapping systems (32). Besides, the large variety of shapes and complexity of historical buildings could affect the precision of the derived urban parameters.

In conclusion, through the analysis of photogrammetric-derived 3D building point clouds, urban density indicators were generated and thus a comprehensive and quantitative view of the urban morphology of Trento.

ACKNOWLEDGMENTS

Authors would like to acknowledge Microgeo (Florenze, Italy) and Riegl (Vienna, Asutria) for the collection of the MMS data in Trento.

REFERENCES

(1) Vinuesa, M.A.T. (1995). Ciudad y patrimonio cultural: el centro histórico de Cuenca. Anales de geografía de la Universidad Complutense, 15, 741-758.
(2) Eguíluz, V. P. (2014). El patrimonio urbano y la planificación. Interpretación de los conjuntos históricos de Castilla y León y sus instrumentos urbanísticos. Ciudades, 17, 221-242. DOI: https://doi.org/10.24197/ciudades.17.2014.221-242
(3) Solis, E., Ureña, J. M., and Mohino, I. (2018). Centralidad territorial y especialización funcional como guía para la intervención en municipios con conjunto histórico. El caso de la Región Urbana Madrileña. ACE: Architecture, City and Enviroment, 13(37), 99-132. DOI: http://dx.doi.org/10.5821/ace.13.37.4904
(4) Tatjer, M. (2000). Las intervenciones urbanísticas en el centro histórico de Barcelona: de la Vía Layetana a los nuevos programas de rehabilitación. Oportunidades de desarrollo sostenible para los conjuntos urbanos históricos. III Jornadas de Geografía Urbana, 13-28.
(5) Valencia, J., Muñoz-Nieto, A., and Rodríguez-González, P. (2015). Virtual modeling for cities of the future. State-of-the art and virtual modeling for cities of the future. State-of-the art and future challenges. The International Archives of Photogrammetry, Remote Sensing and Spatial Information Sciences, XL-5/W4, 179-185. DOI: https://doi.org/10.5194/isprsarchives-XL-5-W4-179-2015
(6) Van Oosterom, P., Stoter, J., and Lemmen, C., (2005). Modelling of 3D cadastral systems. 28th cadastral seminar, 594-606.
(7) González-Aguilera, D., Crespo-Matellan, E., Hernandez-Lopez D., and Rodríguez-González, P. (2013). Automated Urban Analysis Based on LiDAR-Derived Building Models. IEEE Transactions on Geoscience and Remote Sensing, 51 (3), 1844-1851. DOI: https://doi.org/10.1109/TGRS.2012.2205931
(8) Albano, R. (2019). Investigation on Roof Segmentation for 3D Building Reconstruction from Aerial LIDAR Point Clouds. Applied Sciences, 9(21), 4674. DOI: https://doi.org/10.3390/app9214674
(9) Bonczak, B., and Kontokosta, C. E. (2019). Large-scale parameterization of 3D building morphology in complex urban landscapes using aerial LiDAR and city administrative data. Computers, Environment and Urban Systems, 73, 126-142. DOI: https://doi.org/10.1016/j.compenvurbsys.2018.09.004
(10) Shirowzhan, S., Lim, S., Trinder, J., Li, H., and Sepasgozar, S. M. E. (2020). Data mining for recognition of spatial distribution patterns of building heights using airborne lidar data. Advanced Engineering Informatics, 43, 101033. DOI: https://doi.org/10.1016/j.aei.2020.101033
(11) Kaartinen, H. and Hyyppä, J., 2006. Evaluation of building extraction. EuroSDR—project commission 3. Final Report. EuroSDR—European Spatial Data Research.Official Publication. 50, 9-77.
(12) Toschi, I., Ramos, M. M., Nocerino, E., Menna, F., Remondino, F., Moe, K., ... and Fassi, F. (2017). Oblique photogrammetry supporting 3D urban reconstruction of complex scenarios. The International Archives of Photogrammetry, Remote Sensing and Spatial Information Sciences, XLII-1/W1, 519-526. DOI: https://doi.org/10.5194/isprs-archives-XLII-1-W1-519-2017
(13) Wu, B., Wu, S., Li, Y., Wu, J., Huang, Y., Chen, Z., and Yu, B. (2020). Automatic building rooftop extraction using a digital surface model derived from aerial stereo images. Journal of Spatial Science, 1-20. DOI: https://doi.org/10.1080/14498596.2020.1720836
(14) Rong, Y., Zhang, T., Zheng, Y., Hu, C., Peng, L., and Feng, P. (2020). Three-dimensional urban flood inundation simulation based on digital aerial photogrammetry. Journal of Hydrology, Volume 584, 124308. DOI: https://doi.org/10.1016/j.jhydrol.2019.124308
(15) Zhang, T., Huang, X., Wen, D., and Li, J. (2017). Urban building density estimation from high-resolution imagery using multiple features and support vector regression. IEEE Journal of Selected Topics in Applied Earth Observations and Remote Sensing, 10(7), 3265-3280. DOI: https://doi.org/10.1109/JSTARS.2017.2669217
(16) Remondino, F. and Gerke, M., 2015. Oblique Aerial Imagery –A Review. In D. Fristsch (Ed.), Photogrammetric Week (pp. 75-83).
(17) Remondino, F., Toschi, I., Gerke, M., Nex, F., Holland, D., McGill, A., Talaya Lopez, J., Magarinos A., (2016). Oblique aerial imagery from NMA – Some best practices. The International Archives of Photogrammetry, Remote Sensing and Spatial Information Sciences, XLI-I/B4, 639-645. DOI: https://doi.org/10.5194/isprs-archives-XLI-B4-639-2016
(18) Wu, B., Xie, L., Hu, H., Zhu, Q., and Yau, E. (2018). Integration of aerial oblique imagery and terrestrial imagery for optimized 3D modeling in urban areas. ISPRS journal of photogrammetry and remote sensing, 139, 119-132. DOI: https://doi.org/10.1016/j.isprsjprs.2018.03.004
(19) Toschi, I., Remondino, F., Rothe, R., and Klimek, K. (2018). Combining Airborne Oblique Camera and Lidar Sensors: Investigation and New Perspectives. The International Archives of Photogrammetry, Remote Sensing and Spatial Information Sciences, XLII-1, 437-444. DOI: https://doi.org/10.5194/isprs-archives-XLII-1-437-2018
(20) Toschi, I., Nocerino, E., Remondino, F., Revolti, A., Soria, G., and Piffer, S. (2017). Geospatial Data Processing For 3D City Model Generation, Management and Visualization. The International Archives of Photogrammetry, Remote Sensing and Spatial Information Sciences, XLII-1/W1, 519-526. DOI: https://doi.org/10.5194/isprs-archives-XLII-1-W1-527-2017

(21) Rodríguez-Gonzálvez, P., Jiménez Fernández-Palacios, B., Muñoz-Nieto, Á. L., Arias-Sanchez, P., and Gonzalez-Aguilera, D. (2017). Mobile LiDAR system: New possibilities for the documentation and dissemination of large cultural heritage sites. Remote Sensing, 9(3), 189, 17 pp. DOI: https://doi.org/10.3390/rs9030189
(22) Toschi, I., Rodríguez-Gonzálvez, P., Remondino, F., Minto, S., Orlandini, S., and Fuller, A. (2015). Accuracy evaluation of a mobile mapping system with advanced statistical methods. The International Archives of Photogrammetry, Remote Sensing and Spatial Information Sciences, XL-5/W4, 245-253. DOI: https://doi.org/10.5194/isprsarchives-XL-5-W4-245-2015
(23) Bing Maps (6th June 2021). Recovered from: https://www.bing.com/maps
(24) Remondino, F., Spera, M. G., Nocerino, E., Menna, F., and Nex, F. (2014). State of the art in high density image matching. The photogrammetric record, 29(146), 144-166. DOI: https://doi.org/10.1111/phor.12063
(25) Brenner, C. (2010). Building Extraction. In H.-G. Mass and George Vosselman (Eds.), Airborne and Terrestrial Laser Scanning (pp. 169-212). Whittles Publishing.
(26) Terrasolid (6th June 2021). Terrasolid Ltd. Recovered from http://www.terrasolid.com/home.php
(27) CloudCompare (6th June 2021). CloudCompare: 3D point cloud and mesh processing software Open Source Project. Recovered from https://www.danielgm.net/cc/
(28) Zhang, K., Chen, S. C., Whitman, D., Shyu, M. L., Yan, J., and Zhang, C. (2003). A progressive morphological filter for removing nonground measurements from airborne LIDAR data. IEEE transactions on geoscience and remote sensing, 41(4), 872-882. DOI: https://doi.org/10.1109/TGRS.2003.810682
(29) Rusu, R. B., and Cousins, S., (2011). 3D is here: Point Cloud Library (PCL). IEEE international conference on robotics and automation, 1-4. DOI: https://doi.org/10.1109/ICRA.2011.5980567
(30) Gdeisat, M. and Lilley, F., (2012). MATLAB® by Example: Programming Basics. Newnes.
(31) Servizio Catastro Trento (6th June 2021). "Particelle - Poligonali" della Provincia Autonoma di Trento. Recovered from: www.catasto.provincia.tn.it
(32) Nocerino, E., Menna, F., Remondino, F., Toschi, I., and Rodríguez-Gonzálvez, P. (2017, 26 of June). Investigation of indoor and outdoor performance of two portable mobile mapping systems. In Videometrics, Range Imaging, and Applications XIV (pp. 103320I-1-103320I-15). Munich (Germany): SPIE. DOI: https://doi.org/10.1117/12.2270761